Eur. Phys. J. E **24**, 379–384 (2007)
DOI 10.1140/epje/i2007-10249-5

THE EUROPEAN PHYSICAL JOURNAL E

Self-assembly of rod-coil block copolymers from weakly to moderately segregated regimes

N. Sary[1], C. Brochon[2], G. Hadziioannou[2], and R. Mezzenga[1,3,a]

[1] Department of Physics and Fribourg Center for Nanomaterials, University of Fribourg, Ch. Musée 3, CH-1700, Fribourg, Switzerland
[2] Laboratoire d'Ingénierie des Polymères pour les Hautes Technologies, UMR 7165, Université Louis Pasteur, Ecole Européenne de Chimie, Polymères et Matériaux, 25, Rue Becquerel, F-67087 Strasbourg, France
[3] Nestlé Research Center, Vers-Chez-Les-Blanc, CH-1000 Lausanne 26, Switzerland

Received 19 September 2007
Published online: 21 January 2008 –

Abstract. We report on the self-assembly behaviour of two homologue series of rod-coil block copolymers in which, the rod, a π-conjugated polymer, is maintained fixed in size and chemical structure, while the coil is allowed to vary both in molecular weight and chemical nature. This allows maintaining constant the liquid crystalline interactions, expressed by Maier-Saupe interactions, ω, while varying the tendency towards microphase separation, expressed by the product between the Flory-Huggins parameter and the total polymerization degree, χN. Therefore, the systems presented here allow testing directly some of the theoretical predictions for the self-assembly of rod-coil block copolymers in a weakly segregated regime. The two rod-coil block copolymer systems investigated were poly(DEH-p-phenylenevinylene-b-styrene), whose self-assembly takes place in the very weakly segregated regime, and poly(DEH-p-phenylenevinylene-b-4vinylpyridine), for which the self-assembly behaviour occurs under increased tendency towards microphase separation, hereby referred to as moderately segregated regime. Experimental results for both systems are compared with predictions based on Landau expansion theories.

PACS. 61.46.-w Nanoscale materials – 61.30.Vx Polymer liquid crystals – 64.60.Cn Order-disorder transformations; statistical mechanics of model systems

1 Introduction

During the last 25 years many studies have been devoted to the microphase separation of flexible diblock copolymers also named coil-coil block copolymers. More recently, new block copolymers have surfaced bearing mesogenic units or rigid blocks, which confer to these systems a liquid crystalline behaviour [1–4]. Not only these systems are interesting from a fundamental and theoretical point of view, but they have also a high value and potential in applications such as optoelectronics, photovoltaics [5–11], bioapplications [12], sensoring, etc. The mechanisms leading to equilibrium microseparated phases in flexible coil-coil diblock copolymers, which can be either spherical, hexagonal, bicontinuous gyroid or lamellar, are well understood [13–15] and the equilibrium microseparated phases can be explained, in principle, by using only two independent parameters: the volume ratio of each block and the segregation parameter expressed as the Flory-Huggins interaction parameter times the degree of polymerization (χN). The rod-coil block copolymer case is by far more complex, as liquid crystalline behaviour is induced by the presence of a rigid block in the block copolymer backbone, which can compete with or even dominate the classical microseparation arising from the positive enthalpy of mixing of the two different blocks. Further degrees of complexity in self-assembly of rod-coil block copolymer systems arise from intermolecular forces frequently occurring among rod-like polymers: in the cases of rod polymers realized by alpha-helices secondary structures in polypeptides, H-bonding can arise in between contiguous rods; similarly, in π-conjugated polymer rods, π-π interactions may form among closely packed rods [16–18]. Both types of intermolecular forces are expected to greatly affect the phase separation mechanisms. Finally, the strong anisotropy of rod-like blocks introduces large conformational asymmetry effects in rod-coil block copolymers which can have a considerable impact on the perturb self-assembled morphologies compared to coil-coil block copolymers [19]. The steadily increasing number of experimental and theoretical studies devoted to rod-coil block copolymers, has been triggered by the considerable advances in the synthetic

[a] e-mail: raffaele.mezzenga@unifr.ch

routes followed to control their synthesis [5,20–27]. In the present study we have taken advantage of the progress made on synthetic strategies to design rod-coil block copolymers, to synthesize two homologue series of rod-coil block copolymers having, respectively, i) the same π-conjugated rod block, ii) different coil polymers of variable molecular weight. This has allowed comparing rod-coil systems differing essentially for their χ, and thus their tendency to microphase separation χN, while keeping virtually constant in both systems the extent of liquid crystalline interactions, expressed by the Maier-Saupe interactions, ω. As a result, the differences in phase separation mechanisms in the two homologue series can be understood relying on the ratio ω/χ, where solely χ is varying. The synthesis of the first series, poly-(diethylhexyloxy-p-phenylenevinylene)-b-(styrene) block copolymers (PPV-b-PS), was achieved by atom transfer radical polymerization, starting from a PPV macroinitiator. The other block copolymer series, PPV-b-(4-vinylpyridine) (PPV-b-P4VP) was synthesized by anionic polymerization of 4-vinylpyridine and quenching with properly end functionalized PPV [28]. In what follows, the major differences in the self-assembly mechanisms and phase diagrams of these two systems are discussed, and the physics of self-assembly understood based on available Landau-expansion theories [1].

2 Experimental section

2.1 Materials

PPV-PS and PPV-P4VP were synthesized by atom transfer radical polymerization and anionic synthesis, respectively. Details on the synthetic procedures followed can be found in reference [28].

2.2 Morphological investigation

Annealing procedure

PS-PPV block copolymers samples were annealed in a high vacuum (5×10^{-11} bar) oven according to the following procedure: 4 h at 160 °C and finally 72 h at 140 °C. These temperature steps are necessary to erase the thermal history of the samples and to maintain the blend in the temperature region comprised between the glass transition temperature of PS, 100 °C, and the order-disorder transition temperatures (T_{ODT}) of rod-coil mesophases.

PPV-P4VP block copolymers were also annealed, under the same vacuum conditions, in two steps in order to erase the thermal history of the samples and to maintain the blend in the temperature region comprised between the glass transition temperature of P4VP, 140 °C, and the T_{ODT} of the respective mesophases. The temperature steps consisted of 2 h at 220 °C followed by 24 h at 160 °C.

Small- and wide-angle X-ray scattering (SAXS and WAXS)

Small- and wide-angles X-ray scattering (SAXS, WAXS) diffractograms were acquired on an Anton-Paar SAXSess instrument equipped with a Kratky camera. About 10 mg of polymer were solvent-cast on a mica sheet. Temperature was regulated *in situ* up to 200 °C using a homemade sample holder. In the range 150 °C–200 °C, a stable temperature was achieved in the middle of the sample holder after 30 min. All diffractograms at the various isothermal conditions were acquired after one hour temperature equilibration.

Ultramicrotomy

All samples were embedded in a standard four-components epoxy resin (46 wt% Epon 812, 28 wt% (Dodecenyl Succinic Anhydride) DDSA, 25% (Nadic Methyl Anhydride) NMA, 1% (2,4,6-tris (dimethylaminomethyl) phenol) catalyst). In order to avoid diffusion of the resin components into the sample, the resin was pre-cured 90 min at 80 °C before embedding the sample. The sample was finally embedded in the pre-cured epoxy resin, which was cured for 5 h at 70 °C. The samples were then ultramicrotomed on a Reichert-Jung microtome at room temperature. 50 nm thick sections were collected on 600 hexagonal mesh copper grids (EMS T601H-Cu). In PPV-P4VP diblock copolymers, the PPV phase is stained by osmium tetroxide vapor, whereas the staining of the P4VP phase of PPV-P4VP was achieved by exposing collected sections to vapors of iodine for 1 h to 3 h.

Transmission electron microscopy (TEM)

Bright field imaging was performed on a CM100 Philips TEM operated at 80 kV (emission 2). All images were acquired on a SIS Morada CCD camera.

3 Results and discussion

The molecular characteristics of the four different PPV-b-PS (Fig. 1(**1**)) block copolymers and those of the three PPV-b-P4VP (Fig. 1(**2**)) block copolymers synthesized to assess the differences in self-assembly of rod-coil block copolymers of different χ, are reported in Table 1 and Table 2, respectively. For the purposes of the present work,

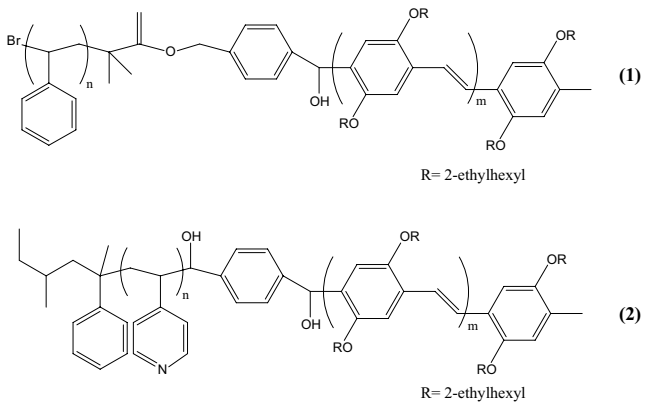

Fig. 1. Molecular structure of (**1**) poly-(diethylhexyloxy-p-phenylene vinylene)-b-(styrene) (PPV-b-PS) and (**2**) poly-(diethylhexyloxy-p-phenylene vinylene)-b-(4-vinylpyridine) (PPV-b-P4VP).

Table 1. Summary of the molecular characteristics of the PPV-PS block copolymers.

	PPV Block		Block copolymer		PS block
	Mn (g/mol) (determined by NMR)	PID	Mn (g/mol) (determined by GPC calibrated with PS standards)	PID	Overall volume fraction
PS52	3400	1.3	5800	1.44	52%
PS56	3400	1.3	6400	1.45	56%
PS65	3400	1.3	8000	1.53	65%
PS82	3400	1.3	22200	1.34	82%

Table 2. Summary of the molecular characteristics of the PPV-P4VP block copolymers.

	PPV block		P4VP block		Block copolymer
	Mn (g/mol) (determined by NMR)	PID	Mn (g/mol) (determined by NMR)	Overall volume fraction	PID
PVP55	4100	1.2	5300	55%	1.40
PVP80	4100	1.2	18300	81%	1.59
PVP88	4100	1.2	31300	88%	1.30

the relatively low molecular weight of the PPV block allows considering it as a perfectly rigid rod. It has in fact been previously reported that the persistence length of the DEH-PPV polymer is of the order of 11 nm [29]. The polymers studied in the present work have overall coil-to-rod ratio ranging from 55% to 88% for PPV-b-P4VP and 52% to 82% for PPV-b-PS, which in the case of an analogue coil-coil block copolymer [13] would be expected to lead to lamellar, hexagonal or spherical morphologies. As anticipated, in the case of rod-coil block copolymers, not only the tendency towards microphase separation, χN, is crucial in understanding the phase separation mechanisms, but also the liquid crystalline interactions associated with the presence of rigid blocks, expressed by the Maier-Saupe constant ω, describing the rod-rod steric repulsion. The relative importance of these two driving forces, quantified by the ratio ω/χ, leads to different microphase-separated morphologies: namely, a large value of ω/χ indicating a predominance of the liquid crystalline behavior may drive a hexagonal or spherical phases into a lamellar-like smectic phase. Since we have intentionally maintained unchanged the rod block in both chemical nature and molecular weight, the Maier-Saupe constant is expected to be identical in both block copolymer series, while the difference in the chemical nature of the coil block is expected to induce a change in the interaction parameter χ.

3.1 Poly(styrene-b-DEH-p-phenylenevinylene)

Because all the PS-PPV block copolymers synthesized exhibit very similar polydispersity index around 1.5, any influence of the polydispersity on the phase segregation can be ruled out *a priori*. Figure 2 shows the characteristic structures observed in the polystyrene-based samples after annealing: a remarkable reduction in the structure order of self-assembled block copolymers is observed as soon as the rod volume fraction is increased. Furthermore, with the exception of PS82, which shows a completely amorphous phase, as also confirmed by the complete lack of birefrengency under cross-polarized optical microscopy, all the other systems present a lamellar-like, structure. The long-range order of the lamellar structure depends directly on the volume fraction of the coil, higher fraction corresponding to the observation of lamellar-like clusters in a homogeneous matrix, and lower coil fraction corresponding to long-range lamellar structures. Thus, contrary to what would have been expected in coil-coil systems, neither intermediate cylindrical or spherical phases are observed in between purely isotropic and lamellar phases. This lack of intermediate microphase-separated morphologies is consistent with a low tendency toward phase segregation. Figure 3 reports the medium-angle X-ray scattering data for the same series of samples reported in Figure 2. Again, with the exception of the block copolymer exhibiting an isotropic phase, the X-ray diffraction patterns of all the other polymers show a sharp peak at $6.5\,\mathrm{nm}^{-1}$. In a previous work, we have demonstrated that the presence of this peak at $6.5\,\mathrm{nm}^{-1}$ is associated with liquid crystallinity of the system, and more precisely, that it corresponds to the close packing of the PPV rods arranged in a smectic C phase [16]. The presence of the PPV close packing, in all but PS82 samples, is the signature of strong Maier-Saupe interactions. At the same time, the absence of transitions structure between smectic and isotropic phase and the severe loss of organization as the coil fraction is increased by a few percents reveal very low interaction parameter χ between PS and PPV. This

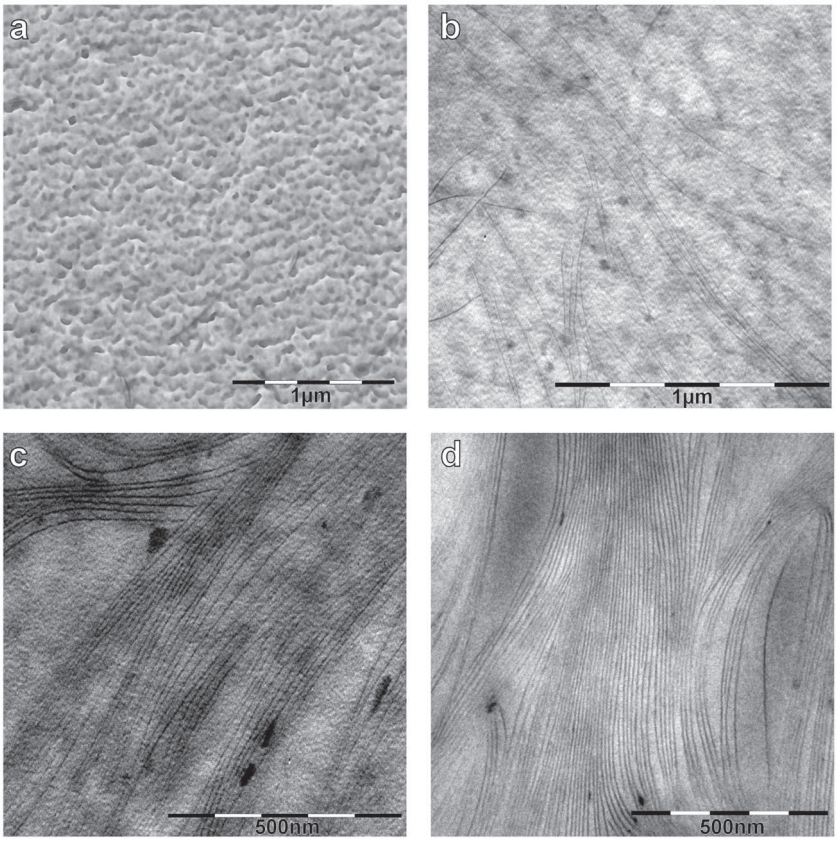

Fig. 2. TEM micrographs of the four different PPV-PS block copolymer systems considered: a) PS82, b) PS65, c) PS56, d) PS52. The structure is becoming progressively more defined when the coil volume fraction is decreased below 65%.

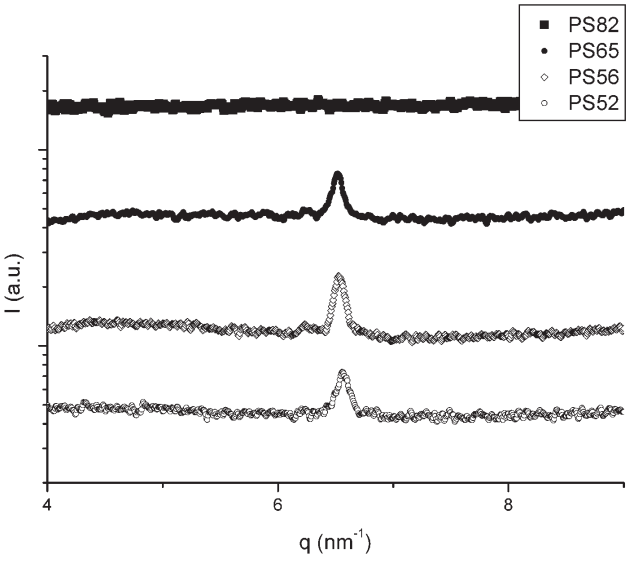

Fig. 3. Medium-angle X-ray diffractograms for the PPV-PS block copolymer systems considered. With the exception of PS82, all the other block copolymers exhibit a peak at $6.5\,\mathrm{nm}^{-1}$, characteristic of the rod-rod close packing.

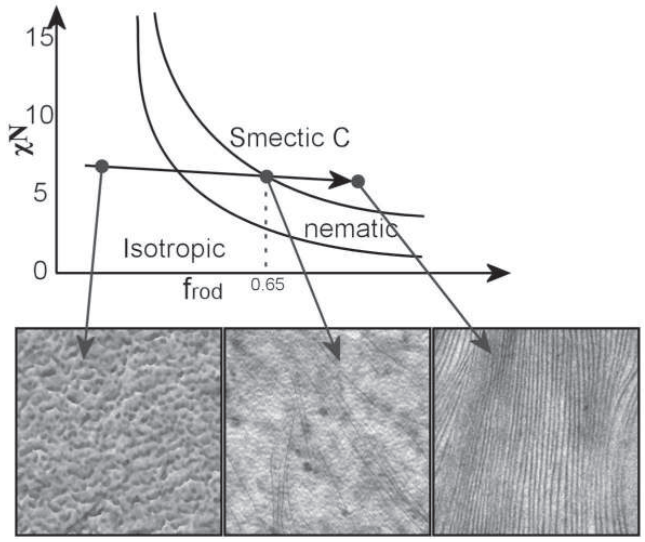

Fig. 4. Comparison between the phase diagram predicted by Landau expansion theories for rod-coil block copolymers with high ω/χ ratios and the microphase separated morphologies experimentally observed for PPV-PS block copolymers. The theoretical phase diagram is redrawn from reference [1].

low value of the Flory-Huggins parameter between PS and PPV is indeed expected to be based on purely chemical similarities between the two blocks. In summary, the relative high values of rod-rod liquid crystalline interactions as well as the low Flory-Huggins parameter between PS and PPV result in a system with a low χ/ω ratio, meaning

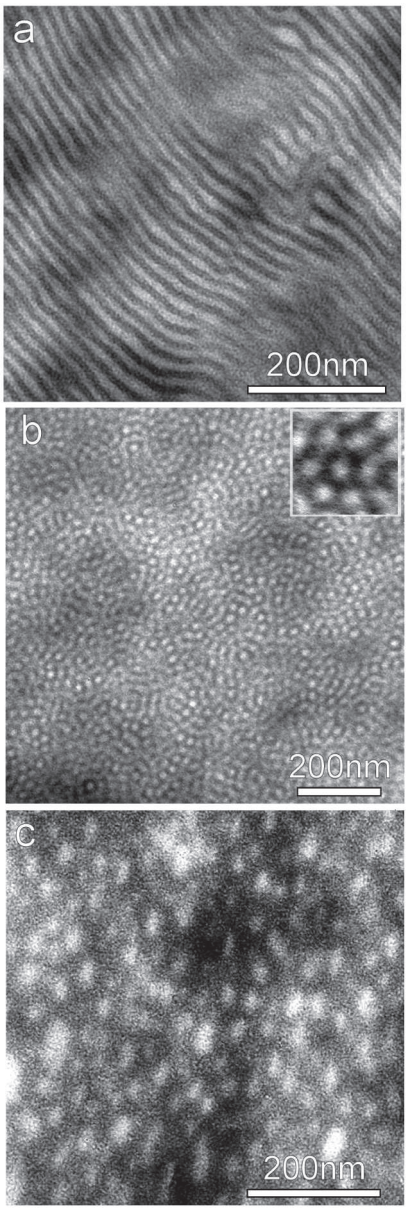

Fig. 5. Typical TEM micrographs for the PPV-P4VP block copolymers studied after selective staining of the P4VP block by iodine (a) PVP55, b) PVP80 and c) PVP88).

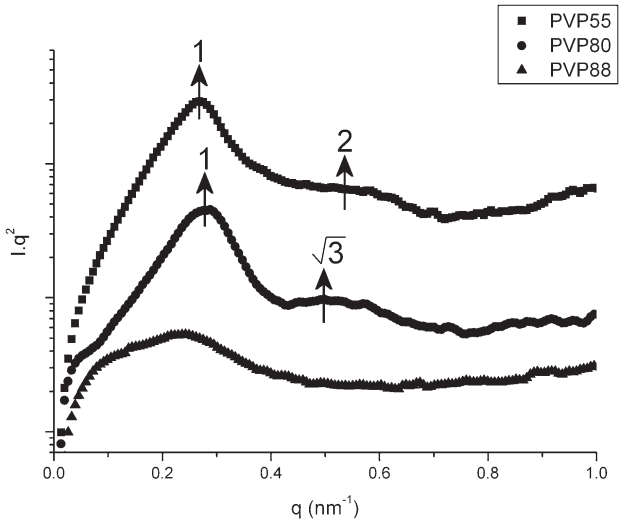

Fig. 6. SAXS diffractograms for the different PPV-P4VP block copolymers considered.

that the structure formation is mainly driven by the liquid crystalline interactions. Figure 4, readapted from reference [1], shows the theoretical phase diagram calculated by Landau-expansion theories for rod-coil block copolymer systems with low χ/ω ratio, and compares it with the structures observed in the present work for PS-PPV block copolymers. As can be observed, only three types of thermodynamic stable phases are expected: smectic C, nematic and isotropic. Therefore, apart from a very narrow nematic region, a direct isotropic-lamellar transition is observed, which is consistent with our experimental evidence. We further note, here, that no evidence of nematic phase has been observed in the series of PS-PPV we have synthesized. A more systematic variation of coil volume fraction between 82% and 65% might be necessary to assess this point.

3.2 Poly(4-vinylpyridine-b-DEH-p-phenylenevinylene)

Figure 5 and Figure 6 show the TEM micrographs as well as the small-angle X-ray diffraction patterns of PVP55, PVP80 and PVP88, respectively. Contrary to what was observed in the case of the PS-b-PPV, in the case of the P4VP-b-PPV the variation of the coil volume fraction does not induce a loss of the microphase separated structure but rather systematic modification of the morphology: the block copolymer successively self-assembles into lamellar, hexagonal and spherical phases, as soon as the coil volume fraction is increased from 55% to 88%. The lamellar phase observed on the TEM micrographs of PVP55 is confirmed by the SAXS diffractograms on which two reflections are visible at $q_1 = 0.32\,\mathrm{nm}^{-1}$ and $q_2 = 0.66\,\mathrm{nm}^{-1}$, the ratio of which, $q_1 : q_2 = 1 : 2$ is compatible with a lamellar structure of period 20 nm. The PVP80 TEM micrograph (Fig. 5b) shows a short-range ordered hexagonal structure, further supported by the two peaks observed on the corresponding SAXS diffraction patterns at $q_1 = 0.26\,\mathrm{nm}^{-1}$ and $q_2 = 0.45\,\mathrm{nm}^{-1}$ (ratio $1 : \sqrt{3}$). Finally PVP88 undergoes phase segregation into a poorly ordered spherical morphology. At room temperature, among all PPV-P4VP systems reported here, only the PVP55 exhibits the X-ray diffraction pattern (not shown here) typical of systems characterized by rod-rod close packing, in close analogy with PS52, PS55 and PS65 PPV-b-PS block copolymer systems. This peak is however disappearing when the sample is heated to 180 °C whereas the lamellar structure remains globally unchanged until 220 °C. This is consistent with a smectic-to-lamellar order-to-order transition at 180 °C. The possibility of switching from smectic to lamellar structures depending on temperature, suggests that microphase segregation tendency and liquid crystalline behavior are relatively equilibrated, and

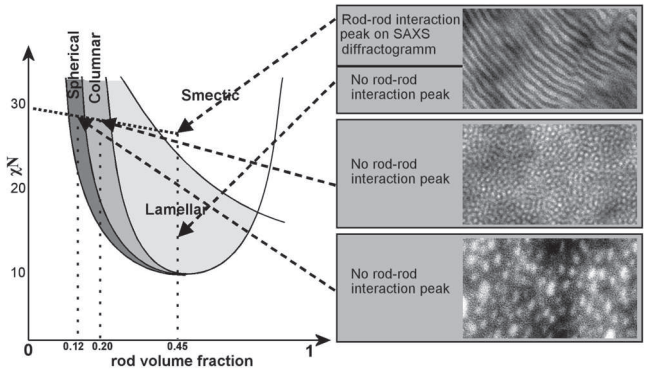

Fig. 7. Comparison between the phase diagram predicted by Landau expansion theories for rod-coil block copolymers with ω/χ ratio of the order of 1 and the microphase separated morphologies experimentally observed for P4VP-PS block copolymers. The theoretical phase diagram is redrawn from reference [1].

thus, that $\omega/\chi \sim 1$. Since ω is virtually unchanged in the two homologue block copolymer systems considered, this is consistent with an increased Flory-Huggins parameter for PPV-P4VP compared to PPV-PS, as can be expected by the increased chemical dissimilarity between PPV and P4VP. A schematics of the phase diagram theoretically expected by Landau expansion theories for systems with balanced microphase and liquid crystalline behaviors, is redrawn from references [1,28] in Figure 7. Remarkably, all the major thermodynamically stable phases predicted theoretically are observed experimentally, and their location in the phase diagram is in excellent agreement with theoretical predictions.

4 Conclusions

We have discussed the self-assembly behavior of rod-coil block copolymer systems in both weakly and moderately segregated regimes. Two homologue series of rod-coil block copolymer systems having the same rod block, and thus the same Maier-Saupe liquid crystalline interactions, but different coils, and therefore Flory-Huggins interaction parameters between rod and coils, have been synthesized and studied. Upon coil volume fraction increase, the weakly segregated system, PPV-PS, exhibited a sharp transition from smectic C to isotropic phase, while the moderately segregated system, PPV-P4VP, underwent transitions from lamellar to hexagonal to spherical phases. Direct comparison of the self-assembly behavior of the two homologue series has allowed to give insight on the interplay of microphase separation tendency and liquid crystalline interactions in the self-assembly of rod-coil block copolymers. The experimental findings of the present work are in excellent agreement with the Landau expansion theoretical predictions by Rendeers and Ten Brinke for self-assembly of rod-coil block copolymer systems.

The authors thank the Swiss Science National Foundation and BASF Aktiengesellschaft for financial support.

References

1. M. Reenders, G. ten Brinke, Macromolecules **35**, 3266 (2002).
2. M.W. Matsen, C. Barrett, J. Chem. Phys. **109**, 4108 (1998).
3. V. Pryamitsyn, V. Ganesan, J. Chem. Phys. **120**, 5824 (2004).
4. A. Halperin, Macromolecules **23**, 2724 (1990).
5. B. de Boer, U. Stalmach, P.F. van Hutten, C. Melzer, V.V. Krasnikov, G. Hadziioannou, Polymer **42**, 9097 (2001).
6. R.H. Friend, R.W. Gymer, A.B. Holmes, J.H. Burroughes, R.N. Marks, C. Taliani, D.D.C. Bradley, D.A. Dos Santos, J.L. Bredas, M. Logdlund, W.R. Salaneck, Nature **397**, 121 (1999).
7. C.J. Brabec, N.S. Sariciftci, J.C. Hummelen, Adv. Funct. Mater. **11**, 15 (2001).
8. N.S. Sariciftci, D. Braun, C. Zhang, V.I. Srdanov, A.J. Heeger, G. Stucky, F. Wudl, Appl. Phys. Lett. **62**, 585 (1993).
9. X.J. Zhang, S.A. Jenekhe, Macromolecules **33**, 2069 (2000).
10. S.S. Sun, Sol. Energy Mater. Sol. Cells **79**, 257 (2003).
11. M.M. Alam, S.A. Jenekhe, Chem. Mater. **16**, 4647 (2004).
12. X.X. Kong, S.A. Jenekhe, Macromolecules **37**, 8180 (2004).
13. L. Leibler, Macromolecules **13**, 1602 (1980).
14. F.S. Bates, G.H. Fredrickson, Annu. Rev. Phys. Chem. **41**, 525 (1990).
15. F.S. Bates, G.H. Fredrickson, Phys. Today **52**, 32 (1999).
16. N. Sary, R. Mezzenga, C. Brochon, G. Hadziioannou, J. Ruokolainen, Macromolecules **40**, 3277 (2007).
17. T. Yamamoto, D. Komarudin, M. Arai, B.L. Lee, H. Suganuma, N. Asakawa, Y. Inoue, K. Kubota, S. Sasaki, T. Fukuda, H. Matsuda, J. Am. Chem. Soc. **120**, 2047 (1998).
18. T. Yamamoto, H. Suganuma, T. Maruyama, T. Inoue, Y. Muramatsu, M. Arai, D. Komarudin, N. Ooba, S. Tomaru, S. Sasaki, K. Kubota, Chem. Mater. **9**, 1217 (1997).
19. P. Friedel, A. John, D. Pospiech, D. Jehnichen, R.R. Netz, Macromol. Theory Simul. **11**, 785 (2002).
20. W.J. Li, H.B. Wang, L.P. Yu, T.L. Morkved, H.M. Jaeger, Macromolecules **32**, 3034 (1999).
21. V. Francke, H.J. Rader, Y. Geerts, K. Mullen, Macromol. Rapid Commun. **19**, 275 (1998).
22. G.N. Tew, M.U. Pralle, S.I. Stupp, J. Am. Chem. Soc. **121**, 9852 (1999).
23. D. Marsitzky, T. Brand, Y. Geerts, M. Klapper, K. Mullen, Macromol. Rapid Commun. **19**, 385 (1998).
24. M.A. Hempenius, B.M.W. Langeveld-Voss, J. van Haare, R.A.J. Janssen, S.S. Sheiko, J.P. Spatz, M. Moller, E.W. Meijer, J. Am. Chem. Soc. **120**, 2798 (1998).
25. H. Kukula, U. Ziener, M. Schops, A. Godt, Macromolecules **31**, 5160 (1998).
26. H.B. Wang, H.H. Wang, V.S. Urban, K.C. Littrell, P. Thiyagarajan, L.P. Yu, J. Am. Chem. Soc. **122**, 6855 (2000).
27. P. Leclere, V. Parente, J.L. Bredas, B. Francois, R. Lazzaroni, Chem. Mater. **10**, 4010 (1998).
28. N. Sary, L. Rubatat, C. Brochon, G. Hadziioannou, J. Ruokolainen, R. Mezzenga, Macromolecules **40**, 6990 (2007).
29. C.L. Gettinger, A.J. Heeger, J.M. Drake, D.J. Pine, J. Chem. Phys. **101**, 1673 (1994).